An Effective Algorithm for MAED Problems with a New Reliability Model at the Microgrid

Amirreza Naderipour [1], Akhtar Kalam [2,*], Zulkurnain Abdul-Malek [1,*], Iraj Faraji Davoudkhani [3], Mohd Wazir Bin Mustafa [4] and Josep M. Guerrero [5]

1   Institute of High Voltage & High Current, School of Electrical Engineering, Faculty of Engineering, Universiti Teknologi Malaysia, Johor Bahru 81310, Malaysia; namirreza@utm.my
2   College of Engineering and Science, Victoria University, Melbourne 3047, Australia
3   Department of Electrical Engineering, Islamic Azad University, Khalkhal Branch, Khalkhal 31367-56817, Iran; faraji.iraj@gmail.com
4   School of Electrical Engineering, Universiti Teknologi Malaysia, Johor Bahru 81310, Malaysia; wazir@utm.my
5   The Villum Center for Research on Microgrids CROM Department of Energy Technology, Aalborg University, 9220 Aalborg East, Denmark; joz@et.aau.dk
*   Correspondence: akhtar.kalam@vu.edu.au (A.K.); zulkurnain@utm.my (Z.A.-M.)

Abstract: This paper proposes a new framework for multi-area economic dispatch (MAED) in which the cost associated with the reliability consideration is taken into account together with the common operational and emission costs using expected energy not supplied (EENS) index. To improve the reliability level, the spinning reserve capacity is considered in the model as well. Furthermore, the MAED optimization problem and non-smooth cost functions are taken into account as well as other technical limitations such as tie-line capacity restriction, ramp rate limits, and prohibited operating zones at the microgrid. Considering all the above practical issues increases the complexity in terms of optimization, which, in turn, necessitates the use of a powerful optimization tool. A new successful algorithm inspired by phasor theory in mathematics, called phasor particle swarm optimization (PPSO), is used in this paper to address this problem. In PPSO, the particles' update rules are driven by phase angles to essentially ensure a spread of variants across the population so that exploitation and exploration can be balanced. The optimal results obtained via simulations confirmed the capability of the proposed PPSO algorithm to find suitable optimal solutions for the proposed model.

Keywords: microgrid; multi-area economic dispatch (MAED); phasor particle swarm optimization (PPSO); reliability-based MAED; reserve constraints; total pollutant emissions

1. Introduction

Thermal generating units constitute a large fraction of electricity production; therefore, the optimal management of such units in the power system is of high importance [1]. Operation of the power system, usually from one hour to one week, mainly belongs to the short-term scheduling problems such as economic load dispatch (ELD) [2] and unit commitment (UC) [3], in which the focus is on the minimization of the operational cost. Accordingly, plenty of research has been carried out addressing ELD using different optimization techniques [4]. On the other hand, an expansion of the ELD optimization issue is the functional multi-area economic dispatch (MAED) optimization problem [5], whose main goal is to evaluate the power generation of generators in various areas and the power exchange between regions [6]. The overall cost of the power grid will reduce. Therefore, following many operating and network constraints [7], taking into account reserve limits in MAED contributes to the problem of reserve constrained multi-area economic dispatch (RCMAED). In addition, the assessment of overall pollutant emissions in RCMAED leads to the reserve restricted multi-area environmental/economic dispatch RCMAEED question [8].

Inclusion of practical considerations (e.g., the valve-point effect, prohibited operating zones, and ramp-rate limitations) in ELD [9] makes the problem sophisticated, which necessitates applying powerful optimization tools to these sorts of problems. Numerous types of methods, including mathematical and meta-heuristic nature-inspired optimization techniques, have been used to tackle the ELD problem in a way to guarantee the optimal solution [10]. Furthermore, authors in [10] solved the RCMAEED problem using the hybridizing sum-local search optimizer (HSLSO) to obtain the optimal solutions. In this respect, economic emission dispatch for thermal units has been pursued by more advanced evolutionary algorithms such as modulated PSO (MPSO) [11] and honey bee mating optimization (HBMO) [12] to utilize the benefits of a faster convergence rate and searching in a wider space. In [13], a novel approach was used based on harmony search (HS) optimization to deal with various types of ED. A new hybrid optimization using Jaya and TLBO has been proposed in [14]. On the other hand, a flower pollination algorithm (FPA) [15], a novel approach using an improved hybrid Jaya algorithm and gradient search method [16], modified stochastic fractal search (SFS) optimization [17], turbulent flow of water-based optimization (TFWO) [18], a new and effective hybrid cuckoo search algorithm (CSA) [19], artificial bee colony optimization (ABCO) [20], large-scale MAED optimization problems integration with wind power [21], chaotic global ABCO [22], and a novel and effective optimizer using Franklin's and Coulomb's laws theory (CFA) [23] have been proposed. For a more comprehensive review, you can refer to [24].

In addition to the common operational cost [25], which is well investigated in generation scheduling studies, the reliability issue is an important factor for power system operators. Interruption in the electricity supplied should be kept at a minimum level to satisfy the costumers' needs [26]. Therefore, the system spinning reserve amount should be sufficient to provide an acceptable level for reliability [27]. To consider this factor, loss of load probability (LOLP) and expected energy not supplied (EENS) are the most effective and prevalent indexes for reliability assessment. As it is obvious, in modern energy management, after considering the common operational cost, it is necessary to consider reliability as well [28].

To cover the various aspects discussed above, this paper presents a new framework for the multi-area economic dispatch, in which the reliability issue together with other technical restrictions are simultaneously taken into account for the first time [29]. To serve this purpose, the EENS index has been added to the formulation and the associated cost is added to the common operational and emission costs. In the model, various constraints such as prohibited operating zones, ramp rate limitations, spinning reserve, and tie-line transmission line capacities are foreseen regarding non-smooth cost functions of thermal units [30]. This paper proposes a powerful modern algorithm called phasor particle swarm optimization (PPSO) to solve various MAED optimization problems, which can be highlighted as the second big contribution of the current study. In mathematics, this algorithm is inspired by the phasor theory and proposes substituting PSO control parameters with variable functions to make PSO a non-parametric algorithm with simpler calculations [31]. The obtained results of this study reveal the effectiveness of the proposed algorithm.

This paper demonstrates that the PPSO algorithm is straightforward and effective for power flow dispatching in electrical systems. All constraints and limitations of the electrical system, in the present study, are assumed with the emission of pollutant gases. Since PSO is a basic algorithm and has been employed in many studies, this version can be used as a base algorithm. There is always a fast convergence problem with the base algorithm in reaching the optimal solution. This issue has been tackled in the proposed version of the algorithm. On the other hand, selecting the best parameters of the algorithm has always been challenging with the base algorithm. The literature shows that different parameters need to be selected for different functions of the basic algorithm. However, the present paper overcomes this issue by presenting and selecting a phase angle, in which all control parameters of the algorithm are assigned to sine and cosine functions of the selected phase angle.

The rest of the paper is organized as follows: first, the formulations of different MAED optimization problems are presented in Section 2. The formulation and flowchart of the proposed PPSO algorithm are presented in Section 3. The simulation results are presented in Section 4, and finally, Section 5 concludes the paper.

2. MAED Optimization Problems

2.1. Objective Functions

The main objective of various types of MAED in different multi-area power systems is to minimize the total power generation and transmission costs while supplying loads of all the market consumers in all network areas and satisfying electrical transmission capacity constraints, minimum and maximum limits of electrical power generation, and power balance constraints. Minimizing the total pollutant emissions is also one of the objectives that can be considered in MAED. MAED can be expressed in [32]. Given that only real powers (active powers) are considered in solving the economic dispatch problem, power and active power are used interchangeably in this article.

On the other hand, electrical energy generation units are subject to several constraints, including valve-point loading on the objective function of the problem. This constraint causes the objective function to lose its flatness and convert into a sine objective function. There are always several types of fuels with different prices in an energy generation system for feeding electrical energy generation units. Thus, the objective function is transformed into a multi-type objective function. This paper applied these two constraints together to the problem.

2.1.1. Minimizing Operational Cost Considering Reliability Issues

The objective function of the single area economic dispatch problem can be expressed as [33]

$$Min \sum_{n=1}^{N} (F_n(P_n)) \tag{1}$$

where

1: $$F_n(P_n) = \begin{cases} a_{n1}P_n^2 + b_{n1}P_n + c_{n1} + |e_{n1} \times \sin(f_{n1} \times (P_{n,\min} - P_n))|, & fuel\,1, \quad P_{n,\min} \leq P_n \leq P_{n1} \\ \dots \\ a_{nk}P_n^2 + b_{nk}P_n + c_{nk} + |e_{nk} \times \sin(f_{nk} \times (P_{n,\min} - P_n))|, & fuel\,k, \quad P_{nk-1} \leq P_n \leq P_{nk} \\ \dots \\ a_{nk}P_n^2 + b_{nk}P_n + c_{nk} + |e_{nk} \times \sin(f_{nk} \times (P_{n,\min} - P_n))|, & fuel\,k, \quad P_{nk-1} \leq P_n \leq P_{n,\max} \end{cases}$$

2: n is the index of available generation units and N is the number of available generation units.

3: k is the index fuel type and K is the number of fuel types.

4: P_n is the output power of the nth unit and $P_{n,\max}$ and $P_{n,\min}$ are maximum and minimum output power limits of the nth unit, respectively.

5: $a_{nk}P_n^2 + b_{nk}P_n + C_{nk}$ is a quadratic generation cost function for fuel type k of the nth unit.

6: a_{nk}, b_{nk}, and c_{nk} are cost function coefficients of the nth unit for fuel type k.

7: $|e_{nk} \times \sin(f_{nk} \times (P_{n,\min} - P_n))|$ is sinusoidal and the non-smooth fuel cost function due to the VPL effects for fuel type k of the nth unit.

8: e_{nk} and f_{nk} are cost function coefficients of the VPL effects model of the nth unit for fuel type k.

The cost function of MAED must consider the cost of power transmission through transmission lines. Thus, Equation (1) would change as [34]:

$$MinF_T = Min(\sum_{n=1}^{N} (F_n(P_n)) + \sum_{j=1}^{M} (f_j(T_j))) \tag{2}$$

where M is the number of transmission lines, f_j is the cost function associated with the jth line, and T_j is the active power flow through the jth line.

As previously mentioned, consideration of reliability in the MAED is the main goal of this paper. In most cases, loss of load probability (LOLP) and expected energy not supplied (EENS) indices are taken into account, as the most well-known reliability indices, for reliability assessment. Indeed, the former models the failure probability of the system [28], while the latter implies the concept of basic energy not supplied. This paper includes the EENS index in the objective function. Therefore, the objective function (2) can be updated as (3). In addition, EENS is formulated through Equations (4)–(9) [20].

$$Min\ F_T = Min\left(\sum_{n=1}^{N}(F_n(P_n)) + \sum_{j}^{M}(f_j(T_j)) + EENS \times c_{ens} \right) \tag{3}$$

$$EENS = \sum_{lp=1}^{LP} \left(EPNS_{lp} \times TD_{lp} \right) \tag{4}$$

$$EPNS_{lp} = \begin{cases} Probability_{lp} \times \left(P_{lp}^L - P_{lp}^G \right) & P_{lp}^L > P_{lp}^G \\ 0 & P_{lp}^L \le P_{lp}^G \end{cases} \tag{5}$$

$$Probability_i = \left(\prod_{H' \in X} U_{H'} \right) \times \left(\prod_{H \in Y}(1 - U_H) \right) \tag{6}$$

$$U_n = \frac{FR_n}{FR_n + RR_n} = \frac{MTTR_n}{MTTF_n + MTTR_n} \tag{7}$$

$$T_{Failure,n} = \frac{1}{FR_n} \tag{8}$$

$$T_{Repair,n} = \frac{1}{RR_n} \tag{9}$$

According to Equation (4), EENS is the summation of all the load points of EPNS indices multiplied by their durations (TD_{lp}), which shows the total value of EENS. In addition, TD_{lp} can be obtained from Figure 1. As can be observed, it is simple to obtain the period of two defined load points with their related data as the number of hours that energy usage is equivalent to a certain load level. Furthermore, based on Equation (5), $EPNS_{lp}$ indicates the value of power not supplied at the lp^{th} load point, where P_{lp}^L is the value of load demand at the lp^{th} load point and P_{lp}^G is the total output powers of available generation units at the lp^{th} load point. The $EPNS_{lp}$ value depends on the unavailability of generators, that is $Probability_{lp}$, which is defined by Equation (6), where X/Y is the set of available (unavailable) generation units at the lp^{th} load point. The mentioned probability expresses the concept of generators failure rate and mean time to repair, which are formulated using Equations (8) and (9), respectively.
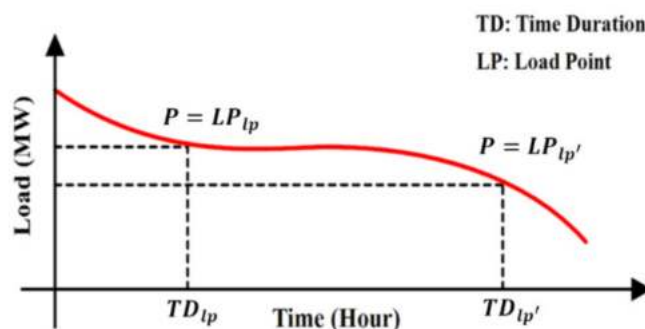

Figure 1. The diagram of load duration.

2.1.2. Minimizing Emissions

One of the issues with electrical energy generation units is the use of fossil fuels. Several types of gases are emitted into the environment when fossil fuels are burnt, hence leading to pollution and destruction of nature. To overcome this problem, designers and engineers consider the emission level of these generation units as an objective function that depends on the generation power of the units during the design and optimization phases. This is formulated as follows [9]:

$$Min\ F_T = Min \sum_{n=1}^{N} E_n(P_n) \tag{10}$$

where

1: $\quad E_n(P_n) = \begin{cases} a_{n1}P_n^2 + \beta_{n1}P_n + \gamma_{n1}, & fuel1, \quad P_{n,\min} \leq P_n \leq P_{n1} \\ \dots \\ a_{nk}P_n^2 + \beta_{n1}P_n + \gamma_{n1}, & fuel\ k, \quad P_{nk-1} \leq P_n \leq P_{nk} \\ \dots \\ a_{nk}P_n^2 + \beta_{nk}P_n + \gamma_{nk}, & fuel\ k, \quad P_{nk-1} \leq P_n \leq P_{n,\max} \end{cases}$

2: $\quad a_{nk}P_n^2 + \beta_{nk}P_n + \gamma_{nk}$ is emission generated by the nth unit for fuel type k.

3: $\quad a_{nk}, \beta_{nk}$, and γ_{nk} are the emission coefficients of the nth unit for fuel type k.

2.2. Constraints

In an energy generation system, designers and engineers always encounter several constraints that need to be satisfied. These constraints depend on the units, transmission lines, system demand level, and the system total loss level. Each of these constraints is provided and formulated.

2.2.1. Area Total Active Power Balance

The total active power balance constraint of area q of the network neglecting the electrical system power losses can be given as [8]

$$\sum_{n=1}^{N_q} (P_n) = \left(P_{Loadq} + \sum_{w \in M_q} T_{qw} \right) \tag{11}$$

where N_q is the number of committed generating units for the qth area, P_{Loadq} is the power demand in the qth area, and M_q is the set of all areas connected to the qth area via a tie-line.

2.2.2. Generator Output Power Limits

The generating capacity of the generator units is constrained to their minimum and maximum limits, as follows [9]:

$$P_{n,\min} \leq P_n \leq P_{n,\max}\ ,\quad i = 1,\dots,N \tag{12}$$

2.2.3. Ramp-Rate Limits

This constraint can be formulated as expressed in (13) [35]:

$$\max(P_{n,\min,} \leq P_n^0 - DR_n \leq P_n \leq \min(P_{n,\max,} \leq P_n^0 + UR_n)) \tag{13}$$

where p_n^0 is the power output of the nth generation unit in the previous stage, and the DR_n and Un_i are ramp-up and ramp-down rate limits of the nth thermal generator, respectively. This constraint determines the lower and upper bounds of the objective variables.

2.2.4. Prohibited Operating Zones (POZ) Due to Physical Operational Limitations

In thermal generating units, the input-output power generation curve with the POZ specifications can be formulated as presented in the following equation [9]:

$$
P_n \in \begin{cases}
P_{n,\min} \leq P_n \leq P_{n1}^1 \\
\dots \\
P_{nh-1}^u \leq P_n \leq P_{nh}^1 \\
\dots \\
P_{nzn}^u \leq P_n \leq P_n^{\max}
\end{cases}
\tag{14}
$$

where h is the index of POZs of the nth unit, zn is the number of POZ in input-output power curve of the nth thermal generating unit, P_{ih}^1 and P_{ih}^u are the minimum and maximum limits of the hth POZ of the nth thermal unit, respectively. In optimization, the optimization variables located in a POZ are set to the lower or upper limit of the POZ, the one closer to their values.

2.2.5. Maximum and Minimum Power Transfer Through Tie-Lines

The tie-line power flow from the qth area to the wth area (T_{qw}) must not violate the maximum tie-line power transfer capacity limit ($T_{qw,\max}$) [8].

$$
|T_{qw}| \leq T_{qw,\max}, \quad w \in M_q
\tag{15}
$$

2.2.6. Spinning Reserve (SR) Requirement in Each Area

In each area, a spinning reserve should be set to encounter the support system adequacy and stability in the case of contingency. Better fulfilment of the necessary SR can be achieved by multi-area reserve sharing [36]. The reserve constraint can be formulated for the qth area as [9]:

$$
\sum_{n=1}^{N_q} S_n + \sum_{w \in M_q} RC_w \geq S_{q,req}
\tag{16}
$$

where $\sum_{n=1}^{N_q} S_n$ is the reserve provided by all the generation units of the qth area, which can be considered as $\sum_{n=1}^{N_q} P_n^{\max} - P_n$, $S_{q,req}$ is the SR requirement in the qth area, and $\sum_{w \in M_q} RC_w$ is the sum of reserves contributed from other areas to the qth area.

2.2.7. Limitation on Power Transfers Considering SR Contribution

The minimum and maximum active power transfer limits through tie-lines must be revised to account for the reserve contribution (RC_{qw}), as follows [36]:

$$
\max\{|T_{qw}|, |T_{qw} + RC_{qw}|\} \leq T_{qw,\max}, \quad w \in M_q
\tag{17}
$$

Therefore, the original objective function of a practical MAEED problem can be amplified by the following equation [9]:

$$
\mathrm{Min}F_T = \mathrm{Min}\left(
\begin{array}{l}
\sum_{n=1}^{N} (F_n(P_n)) + \sum_{j=1}^{M} (f_j(T_j)) + \phi \times \sum_{n=1}^{N} (En(P_n)) + \dots \\
\lambda \times \left| \sum_{N=1}^{N} (P_n) - P_{Load} \right| + \lambda \times (g_1 + g_2)
\end{array}
\right)
\tag{18}
$$

where ϕ is a suitable value selected by the user (in this study: 120), λ is an appropriate penalty coefficient value, and P_{Load} is the entire real load demand in the system. g_1 is $\max(|T_{qw}| - T_{qw,\max}, 0)$ in MAED problem and $\max(\max\{|T_{qw}| - T_{qw} + RC_{qw}\} - T_{qw,\max}, 0)$ in RCMAED and RCMAEED problems. g_2 is 0 for the MAED problem and

$$\sum_{q=1}^{NA} \max(S_{q,req} - \sum_{n=1}^{N_q} S_{nq} - \sum_{w \in M_q} RC_{wq}, 0), \ w \in M_q \text{ for the RCMAED and RCMAEED prob-}$$

lems (NA denotes the number of areas).

3. Phasor Particle Swarm Optimization (PPSO) Technique

This section introduces the original PSO algorithm as well as a number of its common and popular versions. Then, the method proposed and employed in this study, called phasor particle swarm optimization (PPSO), is described.

3.1. Background of Different Variants of PSO

In [37], a review of novel PSO-based algorithms can be found. Each swarm particle in the basic PSO has a current position vector and a current velocity vector. The current position vector of the *i*th particle, for instance, is [23]

$$X_i = [x_{i1}, x_{i2}, \ldots, x_{iD}] \tag{19}$$

and its current velocity vector is [23]

$$V_i = [v_{i1}, v_{i2}, \ldots, v_{iD}] \tag{20}$$

At the start of the optimization process, these vectors are started arbitrarily. With the use of its current position and velocity vectors, the position and velocity of the *i*th particle are updated. In this system, the best position the *i*th particle has experienced so far is the best personal position vector, *Pbest$_i$*, and the best position all particles have experienced so far is the best global position vector, *Gbest*.

The optimization phase is carried out in each iteration of the algorithm based on design knowledge to maximize the objective function (f). In each new iteration, therefore, a new velocity (V_i^{Iter+1}) is generated, using the following equation for d = 1, 2, ... D [24]:

$$v_{id}^{Iter+1} = v_{id}^{Iter} + c_1 \times r_{id}^1 \times (pbest_{id}^{Iter} - x_{id}^{Iter}) + c_2 \times (gbest_{id}^{Iter} - x_{id}^{Iter}) \tag{21}$$

where c_1 and c_2 are acceleration control coefficients, which can be chosen by the designer, $r1_{id}$ and $r2_{id}$ are uniform random coefficients in the range of (0, 1), and Iter is the number of the current iteration.

Particle velocity values, V_i, are constrained to the range defined to prevent particles [8] from travelling out of the issue search room.

Each particle's location is then modified as follows [24]:

$$X_i^{Iter+1} = X_i^{Iter} + V_i^{Iter+1} \tag{22}$$

Using the following equation, the personal best position is updated for each particle [23]:

$$Pbest_i^{Iter+1} = \begin{cases} Pbest_i^{Iter}, if \ f(Pbest_i^{Iter}) \leq f(X_i^{Iter+1}) \\ X_i^{Iter+1}, \ otherwise \end{cases} \tag{23}$$

Using the following equation, the best global population position is updated [23]:

$$Gbest_i^{Iter+1} == \begin{cases} Pbest_i^{Iter}, if > f(Pbest_i^{Iter+1}) \leq f(Gbest^{Iter}) \\ X_i^{Iter}, \ otherwise \end{cases} \tag{24}$$

A modified PSO algorithm (PSO-ω) was introduced by Shi and Eberhartin [24], in which the inertia weight was presented to balance the local and global search. In PSO-ω, each particle's new velocity is calculated as follows [23]:

$$v_{id}^{Iter+1} = \omega^{iter} \times v_{id}^{Iter} + c_1 \times r_{id}^1 \times (Pbest_i^{Iter} - x_{id}^{Iter}) + c_2 \times r_{id}^2 \times (gbest_i^{Iter} - x_i^{Iter}) \tag{25}$$

In [24], the proposed ω is linearly decreased from $\omega_{\max}(=\omega^{iter=1})$ (initial value) to $\omega_{\min}(=\omega^{iter\ \max})$ (final value) during the optimization process as follows [23]:

$$\omega^{Iter} = \omega_{\max} - (\omega_{\max} - \omega_{\min}) \times \frac{Iter}{Iter_{\max}} \qquad (26)$$

The paper proposed 0.9 and 0.4 for $\omega_{\max}$ and $\omega_{\min}$ values, respectively.

An updated PSO algorithm was proposed by Clerc and Kennedy [38] using a new control parameter, called the constriction factor χ, which improves the PSO convergence speed by changing Equation (25) to the one below [38]:

$$v_{id}^{Iter+1} = \chi(v_{id}^{Iter} = +c_1 \times r_{id}^1 \times (Pbest_{id}^{Iter} - x_{id}^{Iter}) + c_2 \times r_{id}^2 \times (gbest_{id}^{Iter} - x_{id}^{Iter})) \qquad (27)$$

It is centered on the control coefficient values $c_1 = c_2 = 2.05$, where the control parameter χ is set to 0.729 using Equation (28) [38]:

$$\chi = \frac{2}{\left| 2 - (c_1 + c_2) - \sqrt{(c_1 + c_2)^2 - 4(c_1 + c_2)} \right|} \qquad (28)$$

In the current paper, a new version of PSO, called phasor particle swarm optimization (PPSO), is suggested, which is motivated by the phasor theory in mathematics. In the suggested PPSO process, all control variables are put in the algorithm-generated step angle θ. This renders the PSO (which has simplified equations) a non-parametric algorithm. In contrast with other algorithms, the best benefits of the proposed PPSO algorithm are the improvement in optimization performance considering the increase in the problem dimension. To solve real-parameter problems, the proposed algorithm, which is defined in the following pages, can be effectively used.

3.2. Parameter Setting in PPSO

In this paper, two periodic trigonometric functions, i.e., $\cos\theta$ and $\sin\theta$, and their absolute values are used to create PSO control parameters. $\cos\theta$ and $\sin\theta$ are periodic functions with a period of 0 to 2π radians (6.2832) and have values in the range of -1 to 1. Periodic functions with periods of π radians and values in the range of 0 and 1 are also their absolute values.

The periodic nature of these functions is used to substitute the phase angle θ for all control parameters of the PSO algorithm and to transform them into θ functions to accomplish various strategies. For this reason, a one-dimensional phase angle, θ_i, is defined for each particle so that, for example, the ith particle could be modelled by a magnitude vector $\vec{X_i}$ with angle θ_i and represented as $\vec{X_i}\angle\theta$.

The periodic nature of these functions is used to replace all control parameters of the PSO algorithm by phase angle θ and to convert them to functions θ to reach different strategies. For this purpose, a one-dimensional phase angle, θ_i, is defined for each particle such that, for example, the ith particle could be modeled by a magnitude vector $\vec{X_i}$ with angle θ_i and represented as $\vec{X_i}\angle\theta$.

The value of ω is set to zero ($\omega = 0$) for the proposed PPSO algorithm, the same as for PSO-TVAC in [39] and even the current model; this approach can, however, be established for other improved PSO algorithms. The suggested particle motion model is as follows [40]:

$$v_i^{Iter} = p(\theta_i^{Iter}) \times (Pbest_i^{Iter} - X_i^{Iter}) + g(\theta_i^{Iter}) \times (Gbest^{Iter} - X_i^{Iter}) \qquad (29)$$

By testing different $p(\theta_i^{Iter})$ and $g(\theta_i^{Iter})$ functions for PPSO on real test functions, the following functions were selected.

The following functions were chosen by evaluating various $p(\theta_i^{Iter})$ and $g(\theta_i^{Iter})$ functions for PPSO on actual test functions [40]:

$$p(\theta_i^{Iter}) = \left| \cos \theta_i^{Iter} \right|^{2*\sin \theta_i^{Iter}} \tag{30}$$

$$g(\theta_i^{Iter}) = \left| \sin \theta_i^{Iter} \right|^{2*\cos \theta_i^{Iter}} \tag{31}$$

It is possible to obtain all the appropriate behaviours and techniques using these $p(\theta_i^{Iter})$ and $g(\theta_i^{Iter})$ functions throughout the running of the algorithm. Often, all of these tasks together raise or decrease and their actions are sometimes inverse.

There is also the probability, in a particular step angle, that these functions become identical to each other. Therefore, it is conceivable that a broad value is achieved by one of the functions. Such behaviours generate adaptive search functions, which are originally produced by control parameters, utilizing only particle-phase angles. This provides a balance between global search and local search, and an adaptive and non-parametric algorithm is converted by the algorithm. These quick or sluggish increases or decreases in the same or opposite direction(s) of $p(\theta_i^{Iter})$ and $g(\theta_i^{Iter})$ enable the algorithm to escape from premature convergence to an ideal local solution.

3.3. Flowchart of PPSO

Figure 2 shows the flowchart of the PPSO algorithm, which is close to other PSO algorithms. First, N_{Pop} random particles (initial population) $\overrightarrow{X_i} = |X_i| < \theta_i$ (i = 1: N_{Pop}) are generated in the D-dimensional space of the problem with their phasor angle θ_i with uniform distribution $\theta_i^{Iter=1} = U(0, 2\pi)$ and with the initial speed limit $v_{max,i}^{Iter=1}$. Then, the velocity of each particle in each iteration of the algorithm is updated with the following equation [40]:

$$v_i^{Iter} = \left| \cos \theta_i^{Iter} \right|^{2*\sin \theta_i^{Iter}} \times (Pbest_i^{Iter} - X_i^{Iter}) + \left| \sin \theta_i^{Iter} \right|^{2*\cos \theta_i^{Iter}} \times (Gbest^{Iter} - X_i^{Iter}) \tag{32}$$

Then, the new position of the particle is updated using the equation presented below:

$$\overrightarrow{X_i}^{Iter+1} = \overrightarrow{X_i}^{Iter} + \overrightarrow{V_i}^{Iter} \tag{33}$$

Next, P_{best} and G_{best} are determined, similar to the original PSO algorithm.

The step angle and overall particle velocity are then modified using the following equations for the next iteration [40]:

$$\theta_i^{Ite+1} = \theta_i^{Iter} + T(\theta) \times (2\pi) = \theta_i^{Iter} + \left| \cos \theta_i^{Iter} \right| + \left| \sin \theta_i^{Iter} \right| \times (2\pi) \tag{34}$$

$$V_{i,max}^{Iter+1} = W(\theta) \times (X_{max} - X_{min}) = \left| \cos \theta_i^{Iter} \right|^2 \times (X_{max} - X_{min}) \tag{35}$$
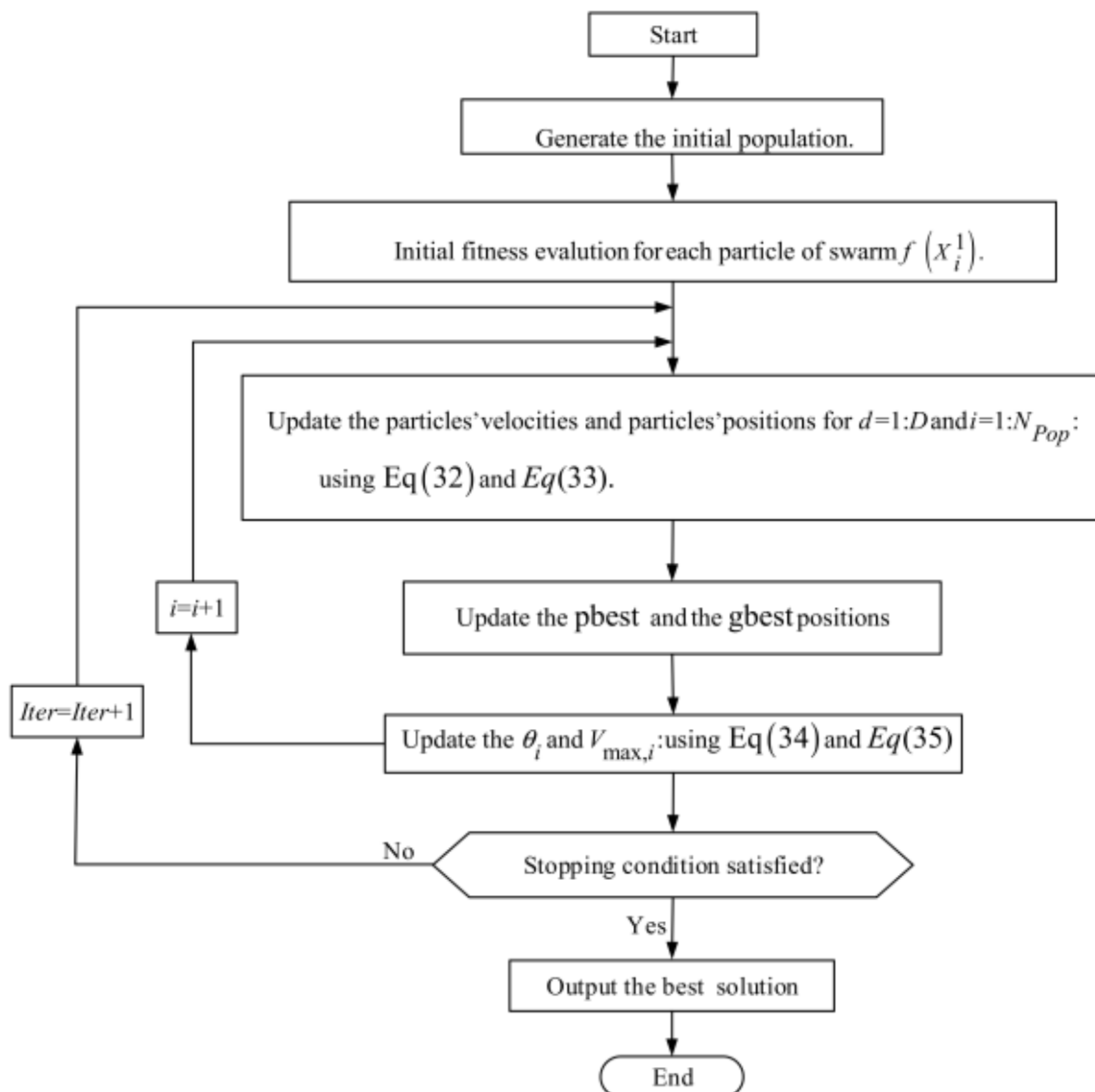
Figure 2. Flowchart of the proposed phasor particle swarm optimization (PPSO) algorithm process.

4. Results and Discussion

4.1. Optimization Results

The proposed PPSO algorithm was evaluated on three case studies of practical MAED problems in three different multi-area power systems: (1) a two-area test power system comprising four electrical power generators as a small-scale test MAED optimization problem, (2) a four-area test power system comprising 16 electrical power generators for MAED, RCMAED, and RCMAEED optimization problems, and (3) a two-area test power system comprising 40 electrical power generators as a large-scale test MAED problem. The results of PPSO were compared with those of previously-improved variants of PSO in the literature such as adaptive PSO (APSO) [41], comprehensive learning PSO (CLPSO) [42], the improved standard PSO 2011 (SPSO2011) [43], fully informed particle swarm (FIPS) [44], and Frankenstein's PSO (FPSO) [45].

4.1.1. The MAED Problems Optimization Process Using PPSO

The steps involved in the algorithm of the proposed PPSO optimizer for solving MAED problems with non-smooth objective functions in multi-area power systems are as follows:

Step 1: Setting the control parameters and the required data of the power system and generation units in the multi-area network.

Step 2: Producing the initial random phasor particle swarm of the PPSO optimizer as follows [9]:

$$P_n^L = \max\{P_{n,\min}, P_n^0 - DR_n\}, P_n^U = \min\{P_{n,\max}, P_n^0 - UR_n\},$$
$$P_n^L \le P_n \le P_n^U \tag{36}$$

$$\left[X_{j,i}^0\right]_{D \times N_{pop}} = \left[P_n^L + rand_{j,n}(0,1) \times (P_n^U - P_n^L)\right]_{D \times N_{pop}} \tag{37}$$

Step 3: Calculating the objective function values of the MAED problem, while imposing constraints of the generation units and multi-area network.

Step 4: Producing a new particle phasor swarm of the PPSO optimizer using Equation (32) to (35).

Step 5: Calculating the objective of the MAED problem.

Step 6: Repeating steps 4 and 5 until the iterations are finished.

4.1.2. Practical MAED Optimization Problems

(a)   The small-scale test system

The under-study system uses fossil fuel; thus, we need to consider the emission levels of units. The small-scale test system is a two-area power system comprising four electrical power generators whose data were extracted from [12,32–34], and its tie-line power flow limit and total power demand are 200 MW and 1120 MW, respectively. The demand in area 1 (comprising units 1 and 2) is 70% of the total demand, and the demand in system area 2 (comprising units 3 and 4) is 30% of the total demand [8]. The best global optimal solution of this test system was obtained using each of the PSO algorithms in 30 separate runs with a maximum number of iterations equal to 100 and maximum population size equal to $N_{Pop} = 80$. This table represents the results of PPSO, APSO, CLPSO, SPSO2011, FPSO, FIPS, PSO-TVAC [8], Hopfield neural network (HNN) method [46], and direct search method (DSM) [47]. Table 1 shows that the minimum operation and fuel cost obtained by the PPSO optimizer was 10,604.6741 ($/H), which was less than that of HNN [46], DSM [47], and PSO-TVAC [8].

Table 1. Comparison of the best solutions obtained for the small-scale test system.

Method	P_1 (MW)	P_2 (MW)	P_3 (MW)	P_4 (MW)	T_{12} (MW)	$\sum P_g$	Cost ($/H)
HNN [46]	-	-	-	-	-	-	10,605
DSM [47]	-	-	-	-	-	-	10,605
PSO-TVAC [8]	444.8047	139.1953	211.0609	324.9391	−200	1120	10,604.68
PPSO	445.1223	138.8778	212.0426	323.9573	−199.9999	1120	10,604.67
APSO	445.3207	138.6794	212.2054	323.7945	−199.9999	1120	10,604.67
CLPSO	445.1213	138.8788	212.0413	323.9586	−199.9999	1120	10,604.67
SPSO2011	445.1223	138.8778	212.0426	323.9573	−199.9999	1120	10,604.67
FPSO	445.0654	138.9347	211.9258	324.0741	−199.9999	1120	10,604.67
FIPS	445.2274	138.7727	211.9977	324.0022	−199.9999	1120	10,604.67

(b)   The medium-scale test system

This medium-scale system is a four-area power system comprising 16 electrical power generators, whose data, including data of power generating units and tie-line minimum and maximum flow limits, were extracted from [48–50]. The power demands are 400 MW in area 1 (comprising units 1 to 4), 200 MW in area 2 (comprising units 5 to 8), 350 MW in area 3 (comprising units 9 to 12), and 300 MW in area 4 (comprising units 13 to 16). The maximum number of iterations and the maximum population size of all PSO algorithms are set to 250 and $N_{Pop} = 80$, respectively. The best global optimal solution obtained by the proposed PPSO optimizer and the best global optimal solutions reported in the literature for the medium-scale test system are presented in Table 2. The global optimal solution to which the proposed PPSO optimizer reached is feasible ($\sum P_g = 1250.0$ MW),

but the best results reported in previous studies using other algorithms, e.g., PSO algorithms, the classical evolutionary programming (CEP) method [51], the hybrid harmony search (HHS) algorithm [48], the network flow programming (NFP) method [52], and the pattern search (PS) algorithm [53] are not feasible. Additionally, the solution obtained by the PPSO optimizer is better than that of the hybridizing sum-local search optimizer (HSLSO) [10] algorithm.

Table 2. The best solutions obtained for the medium-scale test system.

Area No.		PSO [10]	HHS [48]	NFP [52]	CEP [51]	PS [53]	HSLSO [10]	PPSO
1 (400 MW)	P_1 (MW)	150	150	150	150	150	150	150
	P_2 (MW)	100	100	100	100	100	100	100
	P_3 (MW)	67.366	66.86	66.97	68.826	66.971	67.3848	67.31016
	P_4 (MW)	100	100	100	99.985	100	100	100
2 (200 MW)	P_5 (MW)	56.613	57.04	56.97	56.373	56.9718	57.0625	57.07953
	P_6 (MW)	95.474	96.22	96.25	93.519	96.2518	96.1749	96.34877
	P_7 (MW)	41.617	41.74	41.87	42.546	41.8718	41.8472	41.86785
	P_8 (MW)	72.356	72.5	72.52	72.647	72.5218	72.4505	72.53403
3 (350 MW)	P_9 (MW)	50	50	50	50	50.002	50	50
	P_{10} (MW)	35.973	36.24	36.27	36.399	36.272	36.319	36.28298
	P_{11} (MW)	38.21	38.39	38.49	38.323	38.492	38.5911	38.50812
	P_{12} (MW)	37.162	37.2	37.32	36.903	37.322	37.3719	37.26609
4 (300 MW)	P_{13} (MW)	150	150	150	150	150	150	150
	P_{14} (MW)	100	100	100	100	100	100	100
	P_{15} (MW)	57.83	56.9	57.05	56.648	57.051	56.9272	56.9218
	P_{16} (MW)	97.349	96.2	96.27	95.826	96.271	95.8709	95.88068
Tie-line power flow	T_{12} (MW)	0	0	0	−0.018	0	0	0
	T_{13} (MW)	22.588	16.86	18.18	19.587	18.181	17.4643	17.42629
	T_{14} (MW)	−5.176	0	−1.21	−0.758	−1.21	−0.0795	−0.116132
	T_{23} (MW)	66.064	70.61	69.73	68.861	69.73	70.2537	70.51652
	T_{24} (MW)	−0.004	−3.11	−2.11	−1.789	−2.111	−2.7186	−2.686341
	T_{34} (MW)	−100	−100	−100	−99.927	−100	−100	−100
$\sum P_g$ (MW)		1249.95	1249.29	1249.98	1247.995	1249.998	1250	1250
Cost ($/H)		7336.93	7329.85	7337	7337.75	7336.98	7337.03	7337.026

(c) The large-scale test system

The large-scale test system is a two-area power system that has 40 electrical power generators with ramp rate limits, VPL effects, and POZ [8]. The generating units 1 to 20 are in area 1 and generating units 21 to 40 are in area 2. The total power demand is 10,500 MW, from which 7500 MW is the power demand in area 1 and 3000 MW is the power demand in system area 2. The maximum power transfer between the two areas is 1500 MW. Table 3 compares the best global optimal solution obtained using the proposed PPSO optimizer with that of a chaotic differential evolution algorithm (DEC2) [8] and the HSLSO algorithm [10] with a maximum number of iterations equal to 500 and maximum population size equal to $N_{Pop} = 80$. Table 3 shows that the new PPSO optimizer can converge to a better-quality solution in solving a large-scale MAED problem with different practical constraints, whose cost is 125,100.2436 ($/H).

The best, mean, and Std (standard deviation) indexes of the best objective function values for 30 trials of all PSO algorithms for different multi-area power systems are shown in Table 4. Referring to this table and Figure 3, the proposed algorithm has the best standard deviation for the best-obtained solutions. Consequently, it can be claimed that the suggested method is the most reliable method among the methods studied to optimize such problems and also confirms that the PPSO optimizer performance was better than all other algorithms in terms of achieving the optimal solutions of the small-scale MAED optimization problem. It can be seen that the PPSO optimizer provides better quality and more suitable optimal results among all the PSO algorithms.

Table 3. Best solutions obtained for the large-scale test system.

Area 1 (PD = 7500 MW)				Area 2 (PD = 3000 MW)			
Output (MW)	DEC2 [8]	HSLSO [10]	PPSO	Output (MW)	DEC2 [8]	HSLSO [10]	PPSO
P_1	112.8292	110.8012	110.8012	P_{21} (MW)	343.7598	523.2792	523.2794
P_2	114	113.9997	113.9998	P_{22} (MW)	433.5196	523.2791	523.2794
P_3	97.3999	120	120	P_{23} (MW)	523.2794	523.2794	523.2795
P_4	179.7331	179.7331	179.7332	P_{24} (MW)	550	523.2794	523.2794
P_5	97	95.551	95.5504	P_{25} (MW)	550	523.2795	523.2793
P_6	68.0001	140	140	P_{26} (MW)	254	254	254
P_7	300	300	300	P_{27} (MW)	10	10.0001	10
P_8	284.5997	284.5997	284.5997	P_{28} (MW)	10.0001	10	10
P_9	284.5997	284.5997	284.5997	P_{29} (MW)	10	10	10
P_{10}	130	270	270	P_{30} (MW)	47	87.7997	87.7997
P_{11}	360	94	94.0002	P_{31} (MW)	159.7331	188.5959	188.5954
P_{12}	94.0001	300	300	P_{32} (MW)	190	159.7331	159.7331
P_{13}	304.5196	304.5195	304.5195	P_{33} (MW)	163.7269	159.733	159.7331
P_{14}	500	394.2797	394.2793	P_{34} (MW)	164.7998	164.8002	164.8
P_{15}	484.0392	484.0395	484.0395	P_{35} (MW)	200	164.7998	164.7998
P_{16}	500	484.0391	484.0391	P_{36} (MW)	164.7998	164.7998	164.7992
P_{17}	489.2794	489.2794	489.2797	P_{37} (MW)	110	89.1143	89.1143
P_{18}	500	489.2796	489.2794	P_{38} (MW)	57.0571	89.114	89.1142
P_{19}	550	549.9998	549.9998	P_{39} (MW)	25	89.1134	89.1142
P_{20}	550	511.2791	511.2794	P_{40} (MW)	511.2794	242.0001	242
T_{12} (MW)	−1500	−1500	−1500	Cost ($/H)	127,344.9	125,100.3	125,100.2

Table 4. Comparing the simulation final results for the multi-area power systems.

| Test System	Index	FIPS	FPSO	SPSO2011	CLPSO	APSO	PPSO
small-scale system	Best	10,604.6742	10,604.67	10,604.6741	10,604.67	10,604.67	10,604.67
	Mean	10,605.3272	10,604.92	10,604.8543	10,604.68	10,604.73	10,604.67
	Std	1.5275	1.1547	0.5774	0.7022	0.4407	5.75×10^{-5}
	Mean time (s)	4.56	4.78	4	3.16	6.82	2.93
medium-scale system	Best	7341.7942	7340.455	7340.2795	7344.357	7341.714	7337.026
	Mean	7559.7788	7487.087	7637.4443	7486.892	7605.919	7338.115
	Std	74.2674	61.8126	71.271	84.3494	53.07	0.629
	Mean time (s)	20.95	20.67	19.19	18.31	25.57	17.84
large-scale system	Best	128,554.2844	128,128.2	127,085.5386	127,008.9	128,514	125,100.2
	Mean	130,615.4572	129,486	129,414.4588	128,315.4	129,495.4	125,263.2
	Std	1.19×10^3	1.02×10^3	9.84×10^2	2.16×10^2	6.93×10^2	85.3092
	Mean time (s)	54.74	55.85	48.51	48.35	75.3	47.88
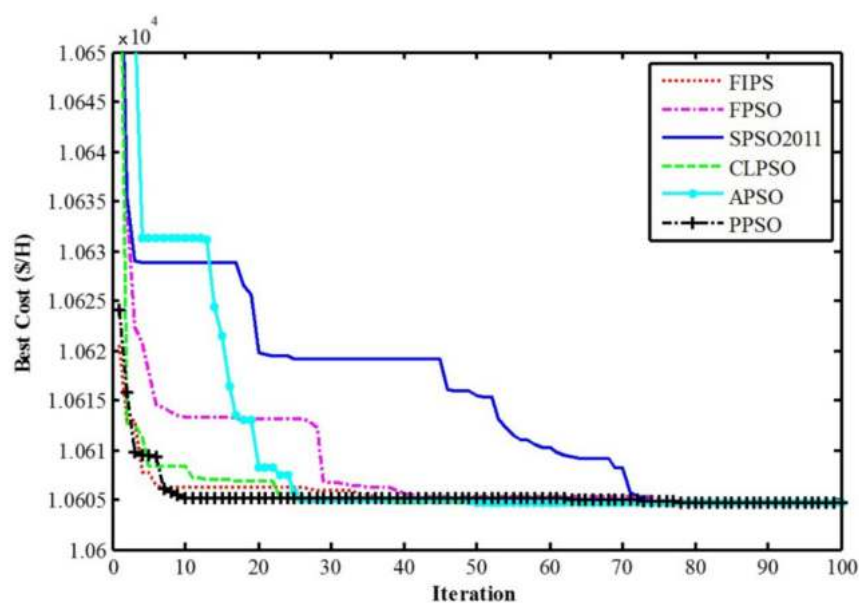
Figure 3. Convergence graphs of different PSO algorithms for the small-scale test system.

Furthermore, the cost function convergence graphs of the PSO algorithms of the multi-area power systems are shown in Figures 4 and 5, which show the superiority of the PPSO optimizer.
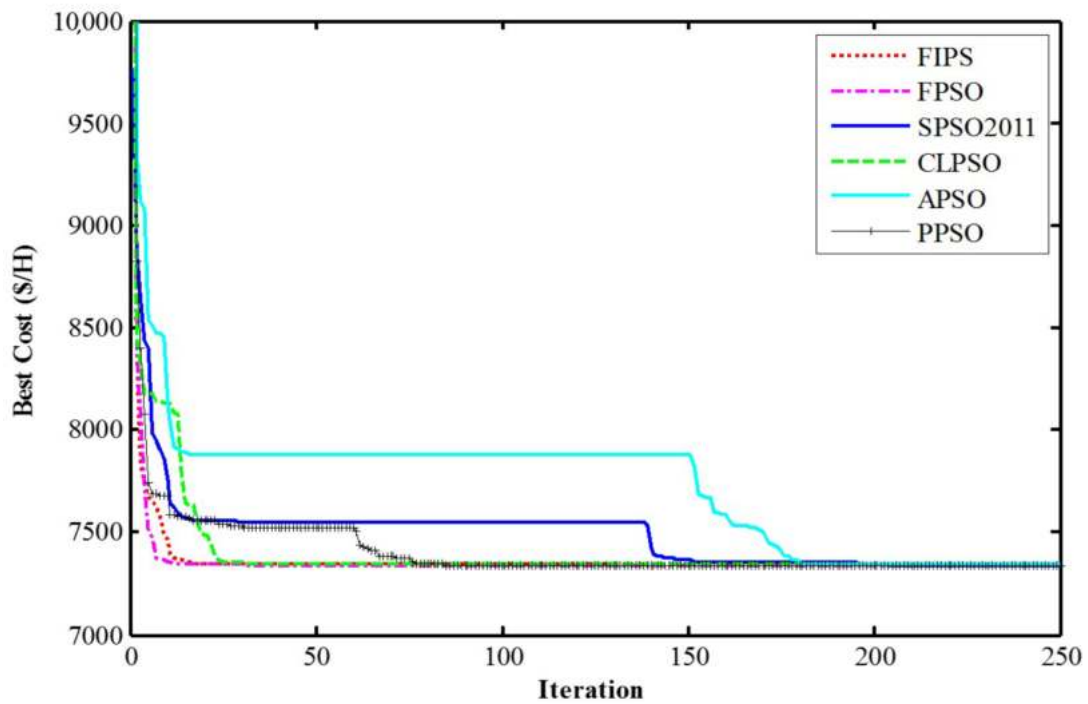

Figure 4. Convergence graphs of different PSO algorithms for the medium-scale test system.
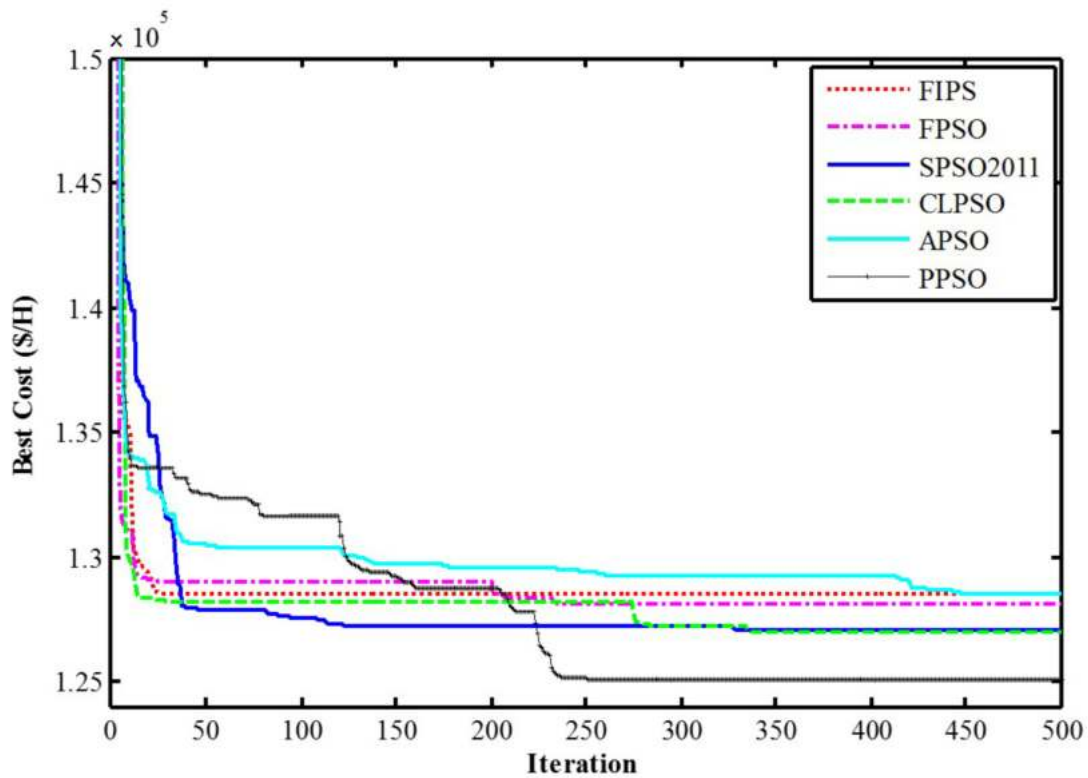

Figure 5. Convergence graphs of different PSO algorithms for the large-scale test system.

4.1.3. RCMAEED and RCMAED Problems

As mentioned before, the medium-scale four-area test power system, previously introduced, was selected for this part of the study. The fuel cost and pollutant emissions objective functions characteristics data and operating constraints of all generating units and tie-line minimum and maximum limits were extracted from [36]. The power demands are 30 MW in the 1st area, 50 MW in the 2nd area, 40 MW in the 3rd area, and 60 MW in the 4th area. The $S_{q,req}$ (SR requirement) for each area is 30% of the area power demand of that area, i.e., 9 MW, 15 MW, 12 MW, and 18 MW for areas 1 to 4, respectively. The maximum number of iterations and maximum population size were set to 500 and N_{Pop} = 120, respectively, and ϕ was also set to 120 for the RCMAEED optimization problem. The global optimal results for the RCMAED and RCMAEED problems obtained using all the PSO optimizers are given in Tables 5 and 6, respectively. The tables show that the best solutions to the RCMAED and RCMAEED problems were obtained by the proposed PPSO optimizer; the optimizer was found to be superior to all other variants of PSO.

Table 5. Optimization results obtained by the PSO optimizers for the RCMAED problem for the four-area power system.

Output (MW)	FIPS	FPSO	SPSO2011	CLPSO	APSO	PPSO
P_1	8.5605	8.7146	8.1347	9.9192	8.468	11.1868
P_2	9.9835	10	8.011	7.259	8.011	9.9596
P_3	11.26	12.3534	13	8.7913	12.7035	6.6997
P_4	0.2616	0.05	1.9639	4.8491	1.605	2.982
P_5	18.807	22.1526	19.5629	23.6046	20.1371	22.8244
P_6	11.261	9.4047	10.9592	9.2998	8.8157	8.8553
P_7	6.1084	3.833	2.1895	3.9163	4.7532	3.9286
P_8	15.2128	17.2551	17.925	16.3556	17.925	17.2481
P_9	4.6622	6.0147	2.9329	6.1264	22.0733	5.8222
P_{10}	10.5192	6.1858	8.5093	0.05	5.3173	0.1993
P_{11}	20.4782	9.1548	23.2033	9.8982	7.4855	9.6888
P_{12}	4.0058	17.2236	5.1026	22.3468	5.1026	22.8171
P_{13}	11	8.1669	9.8282	9.1629	9.8282	8.0614
P_{14}	20	19.7135	17.7366	19.9614	17.7366	19.8021
P_{15}	26.8153	28.7234	30	28.1791	30	29.8714
P_{16}	0.1384	1.2864	0.05	0.0869	0.05	0.0534
P_{17}	0.1275	0.9452	0.5512	0.1	0.5512	0.486
P_{18}	0.3016	0.2525	0.2146	0.2701	0.1433	0.204
P_{19}	0.1	0.18	0.3539	0.3648	0.143	0.138
P_{20}	0.1	1.4402	0.1105	1.4421	0.1105	1.4566
P_{21}	1.1012	1.8441	1.1357	1.84	1.8756	1.8858
P_{22}	0.1	0.1	0.2364	0.1034	0.2364	0.188
RC_{12}	1.6842	2.2985	0.3671	0.6544	2.5336	1.5336
RC_{13}	0.2249	0.1	0.1	0.8206	0.1	0.5945
RC_{14}	1.8788	1.3163	2.1507	0.2931	1.05	0.1674
RC_{23}	0.4049	0.2073	0.1	0.1	1.0058	0.1001
RC_{24}	0.1645	2.4179	1.0183	1.6712	1.0183	2.1473
RC_{34}	0.4582	0.1	0.602	0.2867	0.602	0.3759
Reserve area 1	18.9344	17.882	17.8904	18.1814	18.2125	18.1719
Reserve area 2	23.6108	22.3546	24.3634	21.8237	23.369	22.1436
Reserve area 3	80.3346	81.4211	80.2519	81.5786	80.0213	81.4726
Reserve area 4	33.0463	33.1098	33.3852	33.6097	33.3852	33.2117
Best Cost ($)	2187.418	2178.6024	2188.247	2171.0535	2193.541	2166.377
Mean Cost ($)	2700.367	2634.0676	2461.538	2494.3471	2510.7	2185.794
Std	363.4401	325.6323	204.1498	182.2067	250.0191	13.7298
Time (s)	69.34	66.06	54.48	52.27	77.31	51.93

Table 6. Optimization results obtained by PSO optimizers for the RCMAEED problem for the four-area power system.

Output (MW)	FIPS	FPSO	SPSO2011	CLPSO	APSO	PPSO
P_1	8.2773	10	8.2773	0.05	10.0006	10.0005
P_2	5.444	5.3234	5.444	5.2116	5.3258	5.3259
P_3	6.9757	7.0561	6.9757	12.3788	7.049	7.0491
P_4	7.4634	11.998	7.4634	11.2161	11.9979	11.9978
P_5	21.3822	9.9619	21.3822	16.8448	9.9143	12.2994
P_6	7.3638	11.3019	7.3638	2.117	11.2907	11.3626
P_7	7.6367	14.5624	12.0773	12.9769	14.5612	14.6209
P_8	18	12.6441	14.0655	13.6205	12.7082	10.191
P_9	17.3563	13.2916	17.3563	16.4181	13.2926	13.2921
P_{10}	0.05	0.0891	0.05	0.05	0.0917	0.0919
P_{11}	13.6655	13.0317	13.6655	3.4361	12.6414	12.618
P_{12}	8.1572	14.2427	8.1572	19.1587	14.6307	14.6544
P_{13}	9.2933	4.7521	9.2933	8.7209	4.753	4.7537
P_{14}	12.6671	15.4968	11.2406	12.7486	15.4936	15.4934
P_{15}	17.339	11.813	17.339	11.364	11.8142	11.8143
P_{16}	20.0235	24.4354	20.0235	30	24.4352	24.435
P_{17}	−1.8289	1.19	−1.8289	4.3668	1.1836	1.1836
P_{18}	−2.035	−0.3652	−2.035	−1.7739	−0.3653	−0.3653
P_{19}	1.7937	3.5526	1.0664	−1.7123	3.555	3.555
P_{20}	3.2182	0.1308	3.0699	0.6117	0.1288	0.1288
P_{21}	−2.1972	−0.47	−0.0632	−0.925	−0.4709	−0.4713
P_{22}	0.842	0.4207	0.842	0.8286	0.4199	0.4199
RC_{12}	−2.6122	0.4371	−2.6122	−1.1046	0.4376	0.4355
RC_{13}	1.8735	−3.5706	1.3435	0.4457	−3.4213	−3.396
RC_{14}	3.3365	−5.3328	−10.8828	−7.5176	−5.4329	−4.638
RC_{23}	−2.5379	0.2241	−0.901	2.0858	0.2103	0.2071
RC_{24}	0.6483	−2.7136	0.6483	−1.8365	−2.0113	−3.0807
RC_{34}	−0.5127	−0.6214	−0.5127	−0.2932	−0.7097	−0.6741
Reserve area 1	20.8396	14.6225	20.8396	20.1435	14.6267	14.6267
Reserve area 2	20.6173	26.5297	20.1112	29.4408	26.5256	26.5261
Reserve area 3	80.771	79.3449	80.771	80.9371	79.3436	79.3436
Reserve area 4	31.6771	34.5027	33.1036	28.1665	34.504	34.5036
Cost ($)	2197.8688	2185.4666	2194.0611	2189.6647	2185.0785	2184.0477
Emission (ton)	3.6756	3.4257	3.5176	4.2518	3.4288	3.4097

4.1.4. Reliability-Oriented MAED

As mentioned earlier, reliability is one of the major issues in power system planning and operation. In this study, the cost of energy not supplied (CENS) is investigated as a reliability index in addition to optimizing the operational cost. Table 7 depicts the extracted results of the large-scale test system in the case of considering CENS. The results are different from the case without considering CENS. In this case, the value of ENS is 1.067 (MW); accordingly, the CENS is 7469 ($). Although the operation cost is increased in the case of considering reliability with 2.23%, it is worth mentioning that the ENS value for the case without considering reliability is 2.11 (MW); accordingly, the CENS and total operational cost are 14,770 $ and 139,870.2 $, respectively. In other words, the total operational cost decreased by 3.22%. As a result, solving the proposed problem from the perspective of reliability led to obtaining a solution with an appropriate level of reliability and smaller total operational cost.

Table 7. The obtained values for the proposed reliability-oriented MAED problem for the large-scale test system.

Unit	Output (MW)	Unit	Output (MW)
P_1	114	P_{21}	513.66
P_2	114	P_{22}	513.66
P_3	120	P_{23}	513.66
P_4	180	P_{24}	513.66
P_5	97	P_{25}	513.66
P_6	140	P_{26}	302.097
P_7	300	P_{27}	10
P_8	266	P_{28}	10
P_9	266	P_{29}	10
P_{10}	270	P_{30}	90
P_{11}	126.2842	P_{31}	190
P_{12}	300	P_{32}	188
P_{13}	300	P_{33}	140.55
P_{14}	393.66	P_{34}	152.1113
P_{15}	482.666	P_{35}	148.345
P_{16}	490.1	P_{36}	148.345
P_{17}	481.76	P_{37}	91.55
P_{18}	484.55	P_{38}	91.55
P_{19}	550	P_{39}	91.55
P_{20}	523.9797	P_{40}	267.6017
T12 (MW)			−1500
Operation Cost ($)			127,893.5
CENS ($)			7469
Total Cost			135,362.5

4.2. Discussion

According to the results obtained in this paper, it can be concluded that the proposed algorithm can be a very simple, effective, and widely-used version of the well-known PSO algorithm. Based on the comparisons made between the proposed method and some available PSO algorithms, including adaptive PSO (APSO), comprehensive learning PSO (CLPSO), fully informed particle swarm (FIPS), Frankenstein's PSO (FPSO), and the improved standard PSO 2011 (SPSO2011) as well as several algorithms selected from recently-published papers, e.g., HNN [33], DSM [32], PSO-TVAC [32], PSO [9], HHS [12], NFP [37], CEP [36], PS [38], HSLSO [9], and DEC2 [7], it was concluded that the proposed method can be effectively applied to different problems in the field of energy and engineering optimization. Furthermore, considering the emission of units, reserve load, and system demand, the economic dispatching problem was analyzed practically and comprehensively.

5. Conclusions

Multi-area economic dispatch (MAED) is a very important issue in power systems, which affects the transmission of electrical energy. In this study, the cost associated with system reliability was added to the operational cost of the thermal unit in MAED for the first time. The objective function of the problem comprises three main terms: operational cost, the costs due to reliability, and emission factors. Regarding various types of technical limitations as well as the spinning reserve capacity, the paper proposed a new, improved version of particle swarm optimization (PSO), i.e., the phasor particle swarm optimization (PPSO) algorithm, to tackle complex optimization problems. The algorithm uses phasor theory in mathematics to define a new method for creating PSO control parameters and it was applied to optimal MAED problems in the context of different simulation tests. While in the first test the superiority of the PPSO algorithm was confirmed in terms of quality, reliability, and robustness in comparison to the existing algorithms of PSO, including adaptive PSO (APSO), comprehensive learning PSO (CLPSO), fully informed

particle swarm (FIPS), Frankenstein's PSO (FPSO), and the improved standard PSO 2011 (SPSO2011), the following tests focused on the impact of reliability considerations on the MAED and RCMAEED.

The obtained optimal results revealed that the proposed algorithm is strong and efficient for optimizing power dispatch in energy systems. In addition, it enjoys a special simplicity compared to its counterparts. Furthermore, the application of phasor theory in different types of improved PSO algorithms, including the proposed PPSO, can be further elaborated in different power system optimization problems for future studies.

Conflicts of Interest: The authors declare no conflict of interest.

Abbreviations

Indices:

lp :	Load point index
n :	Committed generation units ϵ $[1, \ldots, N]$
k :	Input fuel types ϵ $[1, \ldots, K]$
j :	Transmission lines ϵ $[1, \ldots, M]$
q, w :	Area's index
d :	Decision variable's index
D :	The number of decision variables
h :	The hth prohibited operating zones (POZ)
H/H'	The H/H'^{th} available/unavailable generation units
M_q :	Set of all areas which are connected to qth area
Parameters:	
N_q :	The number of committed generating units in the qth area
Std :	Standard deviation
zn :	The number of POZs in the nth thermal unit power curve
a_n, b_n, c_n, e_n, f_n :	The fuel cost coefficients of nth thermal unit
$a_{ik}, b_{ik}, c_{ik}, e_{ik}, f_{ik}$:	The fuel cost coefficients of nth thermal unit for kth fuel type
DR_n :	The down ramp rate-limit of nth thermal unit
UR_n :	The up ramp rate-limits of nth thermal unit
P_n^0 :	The power output of nth thermal unit in the first stage
$P_{n,min}$:	The minimum power output of nth thermal unit
$P_{n,max}$:	The maximum power output of nth thermal unit
$P_{nk,min}$:	The minimum power output of nth thermal unit for kth fuel type
P_{nk} :	The maximum power output of nth thermal unit for kth fuel type
P_{nh}^l :	The lower bound for prohibited zone k of nth thermal unit
P_{nh}^u :	The upper bound for prohibited zone k of nth thermal unit
P_{Load} :	System total load demand
P_{Loadq} :	The power demand in qth area
$T_{qw, max}$:	The maximum capacity of the tie-line between qth and wth areas

$\alpha_{nk}, \beta_{nk}, \gamma_{nk},$:	The emission coefficients of nth thermal unit for kth fuel type
$S_{q, req}$:	The spinning reserve requirement in the qth area
φ :	User defined weighting factor for emission cost (in this study: 120)
λ :	Penalty coefficient value
N_{Pop} :	Number of initial population
X_i :	The current position vector of ith particle
V_i :	The current velocity vector of ith particle
$Iter_{max}$:	Maximum number of iterations for PSO algorithm
$Pbest_i$:	The best personal position vector of ith particle
$Gbest$:	The global best position vector
θ :	The phase angle
c_{ens} :	The cost of energy not supplied (7 \$/kWh)
$EPNS_{lp}$:	Expected power not supplied at lpth load point
TD_{lp} :	The time duration of lpth load point
$Probability_{lp}$	The probability of availability and unavailability of generation
X/Y	The set of available (unavailable) generation units
FR_n	The failure rate of nth generator
RR_n	The repair rate of nth generator
$MTTR_n$	Mean time to repair nth generator
$MTTF_n$	Mean time to failure of nth generator
$T_{Failure,n}$	Failure time of nth generator
$T_{Repair,n}$	Repair time of nth generator
U_n	Unavailability (force outage rate) of nth generator

Functions and Variables:

F_T	Objective function
$F_n(P_n)$:	The fuel cost function of nth thermal unit
P_n :	The power output of nth thermal unit
f_j :	Cost function associated with jth transmission line
T_j :	Active power flow through jth transmission line
T_{qw} :	The power flow from qth area to wth area
$E_n(P_n)$:	The emission function of nth thermal unit
RC_{wq} :	The amount of reserve contributed between qth and wth areas
S_n	The reserve provided by all thermal units in the nth area

Abbreviations:

APSO:	Adaptive PSO
CEP:	Classical evolutionary programming
CENS	Cost of energy not supplied
CLPSO:	Comprehensive learning PSO
DEC2:	Chaotic DE/2 algorithm
DSM:	Direct search method
EENS:	Expected energy not supplied
ELD:	Economic load dispatch
EP:	Evolutionary programming
FIPS:	Fully informed particle swarm
FPSO:	Frankenstein's PSO
HNN:	Hopfield neural network
HS:	Harmony search
HSLSO:	Hybridizing sum-local search optimizer
LOLP:	Loss of Load Probability
MAED:	Multi-area economic dispatch
NFP:	Network flow programming
POZ:	Prohibited operating zones
PPSO:	Phasor particle swarm optimization
PS:	Pattern search
PSO:	Particle swarm optimization
PSO-cf:	Modified PSO by constriction factor
PSO-TVAC:	Self-organizing hierarchical particle swarm optimizer with time-varying acceleration coefficients

PSO-ω:	Modified PSO by the inertia weight
RCMAED:	Reserve constrained multi-area economic dispatch
RCMAEED:	Reserve constrained multi-area environmental/economic dispatch
SPSO2011:	The improved standard PSO 2011
SR:	Spinning reserve
VPL:	Valve-point loading

References

1. Naderipour, A.; Abdul-Malek, Z.; Nowdeh, S.A.; Ramachandaramurthy, V.K.; Kalam, A.; Guerrero, J.M. Optimal allocation for combined heat and power system with respect to maximum allowable capacity for reduced losses and improved voltage profile and reliability of microgrids considering loading condition. *Energy* **2020**, *196*, 117124. [CrossRef]
2. Fu, C.; Zhang, S.; Chao, K.-H. Energy management of a power system for economic load dispatch using the artificial intelligent algorithm. *Electronics* **2020**, *9*, 108. [CrossRef]
3. Fu, B.; Ouyang, C.; Li, C.; Wang, J.; Gul, E. An improved mixed integer linear programming approach based on symmetry diminishing for unit commitment of hybrid power system. *Energies* **2019**, *12*, 833. [CrossRef]
4. Abido, M.A. Multiobjective evolutionary algorithms for electric power dispatch problem. *IEEE Trans. Evol. Comput.* **2006**, *10*, 315–329. [CrossRef]
5. Ren, Y.; Fei, S. The auxiliary problem principle with self-adaptive penalty parameter for multi-area economic dispatch problem. *Algorithms* **2015**, *8*, 144–156. [CrossRef]
6. Nowdeh, S.A.; Nasri, S.; Saftjani, P.B.; Naderipour, A.; Abdul-Malek, Z.; Kamyab, H.; Nowdeh, A.J. Multi-Criteria Optimal Design of Hybrid Clean Energy System with Battery Storage Considering Off- and On-Grid Application. *J. Clean. Prod.* **2020**. [CrossRef]
7. Abdollahi, E.; Wang, H.; Lahdelma, R. An optimization method for multi-area combined heat and power production with power transmission network. *Appl. Energy* **2016**, *168*, 248–256. [CrossRef]
8. Sharma, M.; Pandit, M.; Srivastava, L. Reserve constrained multi-area economic dispatch employing differential evolution with time-varying mutation. *Int. J. Electr. Power Energy Syst.* **2011**, *33*, 753–766. [CrossRef]
9. Yu, J.; Kim, C.-H.; Wadood, A.; Khurshiad, T.; Rhee, S.-B. A novel multi-population based chaotic JAYA algorithm with application in solving economic load dispatch problems. *Energies* **2018**, *11*, 1946. [CrossRef]
10. Ghasemi, M.; Aghaei, J.; Akbari, E.; Ghavidel, S.; Li, L. A differential evolution particle swarm optimizer for various types of multi-area economic dispatch problems. *Energy* **2016**, *107*, 182–195. [CrossRef]
11. Jadoun, V.K.; Gupta, N.; Niazi, K.R.; Swarnkar, A. Modulated particle swarm optimization for economic emission dispatch. *Int. J. Electr. Power Energy Syst.* **2015**, *73*, 80–88. [CrossRef]
12. Ghasemi, A. A fuzzified multi objective interactive honey bee mating optimization for environmental/economic power dispatch with valve point effect. *Int. J. Electr. Power Energy Syst.* **2013**, *49*, 308–321. [CrossRef]
13. Dubey, H.M.; Pandit, M.; Tyagi, N.; Panigrahi, B.K. Wind integrated multi area economic dispatch using backtracking search algorithm. In Proceedings of the 2016 IEEE 6th International Conference on Power Systems (ICPS), New Delhi, India, 4–6 March 2016; pp. 1–6.
14. Mokarram, M.J.; Niknam, T.; Aghaei, J.; Shafie-khah, M.; Catalao, J.P.S. Hybrid optimization algorithm to solve the nonconvex multiarea economic dispatch problem. *IEEE Syst. J.* **2019**, *13*, 3400–3409. [CrossRef]
15. Vijayaraj, S.; Santhi, R.K. Multi-Area economic dispatch using flower pollination algorithm. In Proceedings of the 2016 International Conference on Electrical, Electronics, and Optimization Techniques (ICEEOT), Chennai, India, 3–5 March 2016; pp. 4355–4360.
16. Azizipanah-Abarghooee, R.; Dehghanian, P.; Terzija, V. Practical multi-area bi-objective environmental economic dispatch equipped with a hybrid gradient search method and improved Jaya algorithm. *IET Gener. Transm. Distrib.* **2016**, *10*, 3580–3596. [CrossRef]
17. Lin, J.; Wang, Z.-J. Multi-Area economic dispatch using an improved stochastic fractal search algorithm. *Energy* **2019**, *166*, 47–58. [CrossRef]
18. Ghasemi, M.; Davoudkhani, I.F.; Akbari, E.; Rahimnejad, A.; Ghavidel, S.; Li, L. A novel and effective optimization algorithm for global optimization and its engineering applications: Turbulent Flow of Water-based Optimization (TFWO). *Eng. Appl. Artif. Intell.* **2020**, *92*, 103666. [CrossRef]
19. Nguyen, K.P.; Dinh, N.D.; Fujita, G. Multi-Area economic dispatch using Hybrid Cuckoo search algorithm. In Proceedings of the 2015 50th International Universities Power Engineering Conference (UPEC), Stoke on Trent, UK, 1–4 September 2015; pp. 1–6.
20. Basu, M. Artificial bee colony optimization for multi-area economic dispatch. *Int. J. Electr. Power Energy Syst.* **2013**, *49*, 181–187. [CrossRef]
21. Chen, C.-L.; Chen, Z.-Y.; Lee, T.-Y. Multi-Area economic generation and reserve dispatch considering large-scale integration of wind power. *Int. J. Electr. Power Energy Syst.* **2014**, *55*, 171–178. [CrossRef]
22. Secui, D.C. The chaotic global best artificial bee colony algorithm for the multi-area economic/emission dispatch. *Energy* **2015**, *93*, 2518–2545. [CrossRef]

23. Ghasemi, M.; Ghavidel, S.; Aghaei, J.; Akbari, E.; Li, L. CFA optimizer: A new and powerful algorithm inspired by Franklin's and Coulomb's laws theory for solving the economic load dispatch problems. *Int. Trans. Electr. Energy Syst.* **2018**, *28*, e2536. [CrossRef]

24. Shi, Y.; Eberhart, R. A modified particle swarm optimizer. In Proceedings of the 1998 IEEE International Conference on Evolutionary Computation Proceedings, IEEE World Congress on Computational Intelligence (Cat. No. 98TH8360), Anchorage, AK, USA, 4–9 May 1998; pp. 69–73.

25. Laganà, D.; Mastroianni, C.; Meo, M.; Renga, D. Reducing the operational cost of cloud data centers through renewable energy. *Algorithms* **2018**, *11*, 145. [CrossRef]

26. Chaiyabut, N.; Damrongkulkumjorn, P. Optimal spinning reserve for wind power uncertainty by unit commitment with EENS constraint. In Proceedings of the ISGT, Washington, DC, USA, 19–22 February 2014; pp. 1–5.

27. Khokhar, S.; Zin, A.A.M.; Mokhtar, A.S.; Bhayo, M.A.; Naderipour, A. Automatic classification of single and hybrid power quality disturbances using Wavelet Transform and Modular Probabilistic Neural Network. In Proceedings of the 2015 IEEE Conference on Energy Conversion, CENCON 2015, Johor Bahru, Malaysia, 19–20 October 2015; pp. 457–462.

28. Ajmal, A.M.; Ramachandaramurthy, V.K.; Naderipour, A.; Ekanayake, J.B. Comparative analysis of two-step GA-based PV array reconfiguration technique and other reconfiguration techniques. *Energy Convers. Manag.* **2021**, *230*, 113806. [CrossRef]

29. Naderipour, A.; Abdul-Malek, Z.; Nowdeh, S.A.; Kamyab, H.; Ramtin, A.R.; Shahrokhi, S.; Klemeš, J.J. Comparative evaluation of hybrid photovoltaic, wind, tidal and fuel cell clean system design for different regions with remote application considering cost. *J. Clean. Prod.* **2020**. [CrossRef]

30. Naderipour, A.; Abdul-Malek, Z.; Nowdeh, S.A.; Gandoman, F.H.; Moghaddam, M.J.H. A multi-objective optimization problem for optimal site selection of wind turbines for reduce losses and improve voltage profile of distribution grids. *Energies* **2019**, *12*, 2621. [CrossRef]

31. Naderipour, A.; Abdul-Malek, Z.; Vahid, M.Z.; Seifabad, Z.M.; Hajivand, M.; Arabi-Nowdeh, S. Optimal, reliable and cost-effective framework of photovoltaic-wind-battery energy system design considering outage concept using grey wolf optimizer algorithm—Case study for iran. *IEEE Access* **2019**, *7*, 182611–182623. [CrossRef]

32. Lasemi, M.A.; Assili, M.; Baghayipour, M. Modification of multi-area economic dispatch with multiple fuel options, considering the fuelling limitations. *IET Gener. Transm. Distrib.* **2014**, *8*, 1098–1106. [CrossRef]

33. Roy, P.K.; Hazra, S. Economic emission dispatch for wind–fossil-fuel-based power system using chemical reaction optimisation. *Int. Trans. Electr. Energy Syst.* **2015**, *25*, 3248–3274. [CrossRef]

34. Niknam, T. A new fuzzy adaptive hybrid particle swarm optimization algorithm for non-linear, non-smooth and non-convex economic dispatch problem. *Appl. Energy* **2010**, *87*, 327–339. [CrossRef]

35. Ganjefar, S.; Tofighi, M. Dynamic eNconomic dispatch solution using an improved genetic algorithm with non-stationary penalty functions. *Eur. Trans. Electr. Power* **2011**, *21*, 1480–1492. [CrossRef]

36. Wang, L.; Singh, C. Reserve-Constrained multiarea environmental/economic dispatch based on particle swarm optimization with local search. *Eng. Appl. Artif. Intell.* **2009**, *22*, 298–307. [CrossRef]

37. Jensi, R.; Jiji, G.W. An enhanced particle swarm optimization with levy flight for global optimization. *Appl. Soft Comput.* **2016**, *43*, 248–261. [CrossRef]

38. Clerc, M.; Kennedy, J. The particle swarm-explosion, stability, and convergence in a multidimensional complex space. *IEEE Trans. Evol. Comput.* **2002**, *6*, 58–73. [CrossRef]

39. Ratnaweera, A.; Halgamuge, S.K.; Watson, H.C. Self-Organizing hierarchical particle swarm optimizer with time-varying acceleration coefficients. *IEEE Trans. Evol. Comput.* **2004**, *8*, 240–255. [CrossRef]

40. Ghasemi, M.; Akbari, E.; Rahimnejad, A.; Razavi, S.E.; Ghavidel, S.; Li, L. Phasor particle swarm optimization: A simple and efficient variant of PSO. *Soft Comput.* **2019**, *23*, 9701–9718. [CrossRef]

41. Zhan, Z.-H.; Zhang, J.; Li, Y.; Chung, H.S.-H. Adaptive particle swarm optimization. *IEEE Trans. Syst. Man Cybern. Part* **2009**, *39*, 1362–1381. [CrossRef] [PubMed]

42. Liang, J.J.; Qin, A.K.; Suganthan, P.N.; Baskar, S. Comprehensive learning particle swarm optimizer for global optimization of multimodal functions. *IEEE Trans. Evol. Comput.* **2006**, *10*, 281–295. [CrossRef]

43. Zambrano-Bigiarini, M.; Clerc, M.; Rojas, R. Standard particle swarm optimisation 2011 at cec-2013: A baseline for future pso improvements. In Proceedings of the 2013 IEEE Congress on Evolutionary Computation, Cancun, Mexico, 20–23 June 2013; pp. 2337–2344.

44. Mendes, R.; Kennedy, J.; Neves, J. The fully informed particle swarm: Simpler, maybe better. *IEEE Trans. Evol. Comput.* **2004**, *8*, 204–210. [CrossRef]

45. De Oca, M.A.M.; Stutzle, T.; Birattari, M.; Dorigo, M. Frankenstein's PSO: A composite particle swarm optimization algorithm. *IEEE Trans. Evol. Comput.* **2009**, *13*, 1120–1132. [CrossRef]

46. Yalcinoz, T.; Short, M.J. Neural networks approach for solving economic dispatch problem with transmission capacity constraints. *IEEE Trans. Power Syst.* **1998**, *13*, 307–313. [CrossRef]

47. Chen, C.-L.; Chen, N. Direct search method for solving economic dispatch problem considering transmission capacity constraints. *IEEE Trans. Power Syst.* **2001**, *16*, 764–769. [CrossRef]

48. Fesanghary, M.; Ardehali, M.M. A novel meta-heuristic optimization methodology for solving various types of economic dispatch problem. *Energy* **2009**, *34*, 757–766. [CrossRef]

49. Pandit, M.; Srivastava, L.; Pal, K. Static/Dynamic optimal dispatch of energy and reserve using recurrent differential evolution. *IET Gener. Transm. Distrib.* **2013**, *7*, 1401–1414. [CrossRef]
50. Soroudi, A.; Rabiee, A. Optimal multi-area generation schedule considering renewable resources mix: A real-time approach. *IET Gener. Transm. Distrib.* **2013**, *7*, 1011–1026. [CrossRef]
51. Jayabarathi, V.; Ramachandran, T.G.S. Evolutionary programming-based multiarea economic dispatch with tie line constraints. *Electr. Mach. Power Syst.* **2000**, *28*, 1165–1176. [CrossRef]
52. Zhu, J.; Momoh, J.A. Multi-Area power systems economic dispatch using nonlinear convex network flow programming. *Electr. Power Syst. Res.* **2001**, *59*, 13–20. [CrossRef]
53. Al-Sumait, J.S.; Sykulski, J.K.; Al-Othman, A.K. Solution of different types of economic load dispatch problems using a pattern search method. *Electr. Power Compon. Syst.* **2008**, *36*, 250–265. [CrossRef]